

Stackable 4-BAR Mechanisms and Their Robotic Applications

Hoyul Lee and Youngjin Choi

Abstract—This paper proposes a new planar robotic manipulator using stackable 4-BAR mechanisms for various applications such as a manipulator of surgical robot and a manipulator of field robot. The proposed manipulator has an advantage that all driving actuators can be separated from the mechanical mechanism, in other words, we are able to separate all electrical components such as electrical actuators and wirings from mechanical linkage/joint components in the robotic manipulator. Thus the robotic manipulator including working joints and linkages can be manufactured using one or a few material(s) with light-weight and slim-size. Also, the proposed mechanism does not require the actuators to attach directly to driving joints and it can be independently controlled. In addition, we suggest the kinematic analysis of the proposed manipulator composed of input mechanisms, multiple 4-BAR mechanisms and output mechanisms. Finally, a variety of simulation results and a prototype are suggested to show the effectiveness of the stackable 4-BAR mechanisms.

I. INTRODUCTION

THERE are many examples in which an actuator and hydraulic pump and its control system cannot be directly attached to its driving joint as shown in Fig. 1. Fig. 1(a) and (b) illustrate a robotic arm controlled by a wire-driven mechanism. In Fig. 1, all of the actuator systems are located in the robot body, in order to reduce its size and weight of the robot arm [1]. Recently, wire-driven mechanism has been researching for medical robot applications such as surgical robot arms through small ports (for minimally invasive laparoscopic surgery) in [2,3]. Also, the BigDog using hydraulic actuator system has been proposed because its legs with light-weight and small-size could be designed by separating heavy and large size actuator source from the robotic legs as shown in Fig. 1(c) in [4]. Birglen *et al.* have researched the robotic hands by separating the actuators from the parallel mechanism in [5]. One of the most well known mechatronic system which separates the actuators from the working joint is an excavator as shown in Fig. 1(d). Like these, if the driving actuator is separated from its working joint, then we have some advantages because we do not have to consider the actuating system in the robotic manipulator design in viewpoint of its weight and size.

This work was supported in part by the Mid-career Researcher Program through NRF grant funded by the MEST (No. 2008-0061778), and in part by the Ministry of Knowledge Economy (MKE) and Korea Industrial Technology Foundation (KOTEF) through the Human Resource Training Project for Strategic Technology, and in part by the Ministry of Knowledge Economy (MKE) under the Human Resources Development Program for Convergence Robot Specialists, Republic of Korea.

The authors are with the Department of Electronic, Electrical, Control and Instrumentation Engineering, Hanyang University, Republic of Korea. E-mail: cyj@hanyang.ac.kr

Chinzei *et al.* have suggested a surgical robot that can be used in Magnetic Resonance Imaging (MRI) environment in [6]. For real-time tracking of a target position, the surgical robot should be able to be operated even while imaging. Moreover, the motion of surgical robot must not affect on the quality of real-time images. For these reasons, the surgical robot would be better if it is able to be designed with one non-ferromagnetic material in order to keep a constant quality of MRI images. Actually, it is very difficult for conventional robot system to use in the MRI environment because it contains ferromagnetic components in the linkage, working joints, electrical motors and wirings. The stackable 4-BAR mechanism to be suggested in this paper can be an alternative for the surgical robot system.

To make a small-size, light-weight manipulator, many researchers have mainly used the wire-driven mechanisms and small actuator system in [1,2,3]. However, it has a disadvantage which it cannot structurally support large weight nor operate with high force. For this reason, it is difficult to make a solid manipulator with long-size and multi-DOF using the wire-driven mechanism. By contrast, a parallel mechanism has an advantage that is able to support large weight and operate with high force in [7,8,9,10,11,12]. For example, an LCD panel mounting device has been developed using a parallel mechanism and small motors in [12].

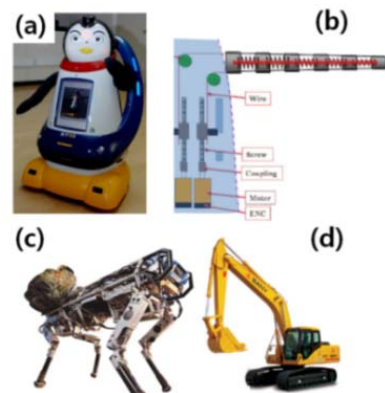


Fig 1. (a) Soft robotic arm [1], (b) Mechanism of spring-backed soft arm [1], (c) BigDog [4], (d) Excavator

As aforementioned, we should select a suitable mechanism for its purpose to design an efficient robotic manipulator, that is, the location of actuators, the material of manipulator and the type of mechanism should be considered according to its working environment. For this, we are to propose a useful

mechanism which is called “stackable 4-BAR mechanism” in this paper. The Fig. 2 shows the concept of 2-DOF robotic manipulator using stackable 4-BAR mechanisms. In detail, the Fig. 2(a) denotes two mechanism planes, in which the first plane has an input and one 4-BAR mechanisms, and the second plane has an input and two 4-BAR mechanisms. Also, each plane is stacked and then bottom links are joined each other and fixed together as shown in Fig. 2(b). Here, we should notice that each mechanism plane has its own input mechanism operated by actuator. An n-DOF robotic manipulator can be similarly suggested by stacking n mechanism planes. The manipulator suggested using 4-BAR mechanisms and input mechanisms has three advantages as follows: first, by separating actuator system from working joint as shown in Fig. 3, we are able to make the working joints small and lightweight, moreover, and it can be made thin if it consists of thin-links. Second, we are able to separate the electrical components such as the electric motors, wirings and sensors from the working joint, thus, the suggested mechanism of working joints can be made only by one material such as steel, glass, wood, plastic, and hard paper. In other words, the stackable mechanism can be applied to the special environment such as the MRI environment. Third, since the suggested mechanism consists of the parallel mechanisms of the 4-BAR, the suggested manipulator is structurally substantial.

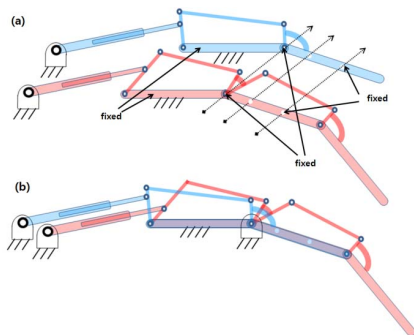


Fig. 2. Concept of stackable 4-BAR mechanism.

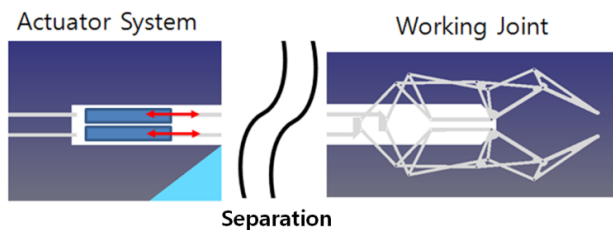


Fig. 3 Advantages of suggested robotic manipulator.

The remaining parts of this paper are as follows; section II and III suggest the kinematic analyses of 1-DOF and n-DOF robotic manipulators to show their controllability; section IV shows the simulations results and prototype of the proposed robot manipulator to show the effectiveness of the stackable 4-BAR mechanisms; section V draws conclusions.

II. 1-DOF MANIPULATOR

In this section, the rate kinematics of a simple 1-DOF manipulator as shown in Fig. 4 is suggested using 4-BAR mechanism. Also, an input mechanism is independently required because the driving actuator is separated from the working joint. To begin with, the rate kinematics of input mechanism is suggested in the following section.

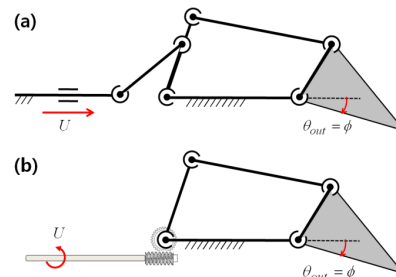


Fig 4. 1 DOF manipulator.

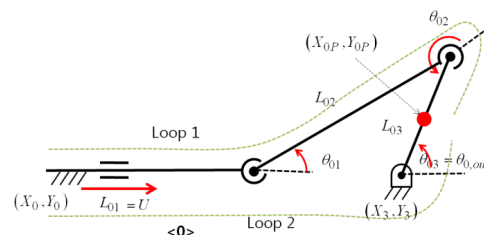


Fig. 5. Kinematics of input mechanism.

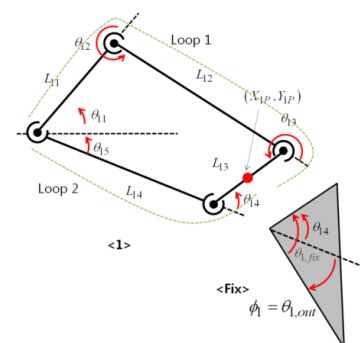


Fig. 6. Kinematics of 4-BAR and output mechanism

A. Input Mechanism

There are two kinds of input mechanism as shown in Fig. 4; the Fig. 4.(a) and (b) show a slide-crank mechanism and the a worm-gear mechanism, respectively. The slide-crank mechanism as shown in Fig. 5 consists of one prismatic joint, three rotary joints and two connecting links. In Fig. 5, $\langle 0 \rangle$ denotes the input mechanism, U is the displacement of linear actuator, θ_{0j} and L_{0j} is j -th joint angle and j -th link length of the input mechanism, $\langle 0 \rangle$, respectively. For instance, θ_{01} is the first joint angle and L_{03} is the third link length of input mechanism, $\langle 0 \rangle$. Let us choose a target point (X_{0P}, Y_{0P}) at the link L_{03} of input mechanism in Fig. 5 to solve the kinematics. The velocity of target point (X_{0P}, Y_{0P}) and the angular

velocity of the link L_{03} can be obtained by differentiating forward kinematics of Loop1 and Loop2 in Fig. 5, respectively, as follows:

$$\begin{bmatrix} \dot{X}_{0P} \\ \dot{Y}_{0P} \\ \dot{\Phi}_{0P} \end{bmatrix} = \begin{bmatrix} 1 & -L_{02}S_{\theta_{01}} - \frac{L_{03}}{2}S_{\theta_{01}+\theta_{02}} & -\frac{L_{03}}{2}S_{\theta_{01}+\theta_{02}} \\ 0 & L_{02}C_{\theta_{01}} + \frac{L_{03}}{2}C_{\theta_{01}+\theta_{02}} & \frac{L_{03}}{2}C_{\theta_{01}+\theta_{02}} \\ 0 & 1 & 1 \end{bmatrix} \begin{bmatrix} \dot{L}_{01} \\ \dot{\theta}_{01} \\ \dot{\theta}_{02} \end{bmatrix} \quad (1)$$

$$\begin{bmatrix} \dot{X}_{0P} \\ \dot{Y}_{0P} \\ \dot{\Phi}_{0P} \end{bmatrix} = \begin{bmatrix} -\frac{L_{03}}{2}S_{\theta_{03}} \\ \frac{L_{03}}{2}C_{\theta_{03}} \\ 1 \end{bmatrix} [\dot{\theta}_{03}] \quad (2)$$

Since Eq. (1) and Eq. (2) denote the velocity relations of same point (X_{0P} , Y_{0P}), it can be represented as follow:

$$\begin{bmatrix} [A_0]_1 & [A_0]_2 & [A_0]_3 \end{bmatrix} \begin{bmatrix} \dot{L}_{01} \\ \dot{\theta}_{01} \\ \dot{\theta}_{02} \end{bmatrix} = [B_0][\dot{\theta}_{03}], \quad (3)$$

where $[A_0]_1$, $[A_0]_2$, $[A_0]_3$ denote first, second and third column vector of 3x3 matrix in Eq. (1). Since the slide-crank mechanism shown in Fig. 5 has one DOF in [9, 10], if the displacement of linear actuator, $U=L_{01}$, is determined, then the remaining three joint angles are calculated. In other words, the L_{01} is an active joint, and θ_{01} , θ_{02} , and θ_{03} are all passive joints. Thus, Eq. (3) can be rewritten for the active joint as

$$\begin{bmatrix} [A_0]_2 & [A_0]_3 & -[B_0] \end{bmatrix} \begin{bmatrix} \dot{\theta}_{01} \\ \dot{\theta}_{02} \\ \dot{\theta}_{03} \end{bmatrix} = [-[A_0]_1][\dot{L}_{01}]. \quad (4)$$

Above Eq. (4) can be also represented as follow:

$$\begin{bmatrix} \dot{\theta}_{01} \\ \dot{\theta}_{02} \\ \dot{\theta}_{03} \end{bmatrix} = [Q_0][\dot{L}_{01}]. \quad (5)$$

From Eq. (5), we can obtain velocity relation between the active joint, L_{01} , and the passive joint, θ_{03} , as following form:

$$[\dot{\theta}_{03}] = [Q_{0(3,1)}][\dot{L}_{01}], \quad (6)$$

where $[Q_{0(3,1)}]$ is the third component of column vector $[Q_0]$.

Now, let us assign the input U and output variables $\dot{\theta}_{0,out}$ of slide-crank mechanism to be L_{01} and θ_{03} in Fig. 5, respectively, then the velocity relation of Eq. (6) between input and output is rearranged as following form:

$$[\dot{\theta}_{0,out}] = [G_0][\dot{U}], \quad (7)$$

where $[G_0] = [Q_{0(3,1)}]$. Till now, the slide-crank mechanism was considered as an input as shown in Fig. 4(a). If the input

is a worm-gear mechanism as shown in Fig. 4(b), then the velocity relation between an input and an output is expressed just by a worm-gear ratio as following form:

$$[G_0] = [r_0], \quad (8)$$

where $[r_0]$ means a gear ratio of the worm-gear.

B. 4-BAR and Output Mechanism

The Fig. 6 illustrates a 4-BAR and output mechanism followed by the input mechanism more detail in 1 DOF manipulator suggested in Fig. 4(a). In Fig. 6, <1> denotes the 4-BAR mechanism and <Fix> denotes the fixed output part. Also, since the link L_{01} of the input mechanism is exactly equal to a link L_{11} of the 4-BAR mechanism, the output joint angle $\theta_{0,out}$ of the input mechanism becomes also equal to an input joint angle θ_{11} of 4-BAR mechanism. Here, we should notice that the general 4-BAR has four joints but we add one joint angle θ_{15} which is determined by the link L_{14} . Actually, the link L_{14} is earthed to the ground in the case of 1 DOF manipulator suggested in Fig. 4(a), but the joint angle θ_{15} of the link L_{14} can be varied in the case of more than 2-DOF manipulator. Thus θ_{11} is an active joint, θ_{15} is a virtual active joint, θ_{12} , θ_{13} , and θ_{14} are passive joints, and $\dot{\Phi}$ is a working joint. Then we can get the velocity relation between input and output of 4-BAR mechanism by the same way that is applied to the slide-crank mechanism as follows:

$$\begin{bmatrix} \dot{\theta}_{12} \\ \dot{\theta}_{13} \\ \dot{\theta}_{14} \end{bmatrix} = [Q_1] \begin{bmatrix} \dot{\theta}_{11} \\ \dot{\theta}_{15} \end{bmatrix} \quad (9)$$

where

$$[Q_1] = [A_1]^{-1}[B_1], \quad (10)$$

$$[A_1] = \begin{bmatrix} -L_{12}S_{\theta_{11}+\theta_{12}} - \frac{L_{13}}{2}S_{\theta_{11}+\theta_{12}+\theta_{13}} & -\frac{L_{13}}{2}S_{\theta_{11}+\theta_{12}+\theta_{13}} & \frac{L_{13}}{2}S_{\theta_{14}+\theta_{15}} \\ L_{12}C_{\theta_{11}+\theta_{12}} + \frac{L_{13}}{2}C_{\theta_{11}+\theta_{12}+\theta_{13}} & \frac{L_{13}}{2}C_{\theta_{11}+\theta_{12}+\theta_{13}} & -\frac{L_{13}}{2}C_{\theta_{14}+\theta_{15}} \\ 1 & 1 & -1 \end{bmatrix} \quad (11)$$

and

$$[B_1] = \begin{bmatrix} L_{11}S_{\theta_{11}} + L_{12}S_{\theta_{11}+\theta_{12}} + \frac{L_{13}}{2}S_{\theta_{11}+\theta_{12}+\theta_{13}} & -L_{14}S_{\theta_{15}} & -\frac{L_{13}}{2}S_{\theta_{14}+\theta_{15}} \\ -L_{11}C_{\theta_{11}} - L_{12}C_{\theta_{11}+\theta_{12}} - \frac{L_{13}}{2}C_{\theta_{11}+\theta_{12}+\theta_{13}} & L_{14}C_{\theta_{15}} & \frac{L_{13}}{2}C_{\theta_{14}+\theta_{15}} \\ -1 & 1 & 1 \end{bmatrix}. \quad (12)$$

From Eq. (9), we can obtain the following relation between (active and virtual joints) inputs and output, θ_{14} :

$$[\dot{\theta}_{14}] = [Q_{1(3,1)} \quad Q_{1(3,2)}] \begin{bmatrix} \dot{\theta}_{11} \\ \dot{\theta}_{15} \end{bmatrix} \quad (13)$$

where $\mathbf{Q}_{1(3,1)}$ and $\mathbf{Q}_{1(3,2)}$ denote (3,1) element and (3,2) element of \mathbf{Q}_1 matrix of Eq. (10), respectively. If the link L_{14} is earthed to ground, Eq. (13) is reduced to:

$$\begin{aligned} \begin{bmatrix} \dot{\theta}_{14} \end{bmatrix} &= \begin{bmatrix} \mathbf{Q}_{1(3,1)} \end{bmatrix} \begin{bmatrix} \dot{\theta}_{11} \end{bmatrix} \\ &= \begin{bmatrix} G_1 \end{bmatrix} \begin{bmatrix} \dot{\theta}_{11} \end{bmatrix} \end{aligned} \quad (14)$$

From Fig. 6, the working joint of 1 DOF manipulator is obtained as follows:

$$\begin{cases} \phi_1 = \theta_{1,out} = \theta_{14} - \theta_{1,fix} \\ \dot{\phi}_1 = \dot{\theta}_{1,out} = \dot{\theta}_{14} \end{cases} \quad (15)$$

Also, Eq. (14) can be rewritten using Eq. (15) as follow:

$$\begin{bmatrix} \dot{\phi}_1 \end{bmatrix} = \begin{bmatrix} G_1 \end{bmatrix} \begin{bmatrix} \dot{\theta}_{11} \end{bmatrix} \quad (16)$$

As a result, the motion of working joint of 1 DOF manipulator can be expressed from the actuator input \mathbf{U} using Eq. (7) and (16) as following form:

$$\begin{bmatrix} \dot{\phi}_1 \end{bmatrix} = \begin{bmatrix} G_1 \end{bmatrix} \begin{bmatrix} G_0 \end{bmatrix} \begin{bmatrix} \dot{\mathbf{U}} \end{bmatrix} \quad (17)$$

where $\begin{bmatrix} G_0 \end{bmatrix}$ and $\begin{bmatrix} G_1 \end{bmatrix}$ are the velocity relations of $\langle 0 \rangle$ and $\langle 1 \rangle$, respectively. In other words, if the actuator input \mathbf{U} is applied to 1 DOF manipulator as shown in Fig. 4, then we can get the working joint angle ϕ_1 from above kinematic relation.

III. MULTI-DOF MANIPULATOR

In this section, we introduce the kinematics of 2-DOF manipulator composed of two mechanism planes as shown in Fig. 7. As a similar way, an N-DOF manipulator consists of N mechanism planes. The Fig. 8 illustrates i -th mechanism plane which consists of the slide-crank as an input and i 4-BARs. In Fig. 8, $\langle i, j \rangle$ means the j -th mechanism of i -th plane, and ${}_i\theta_{jk}$ and ${}_iL_{jk}$ mean k -th link and joint of j -th 4-BAR in the i -th mechanism plane, respectively.

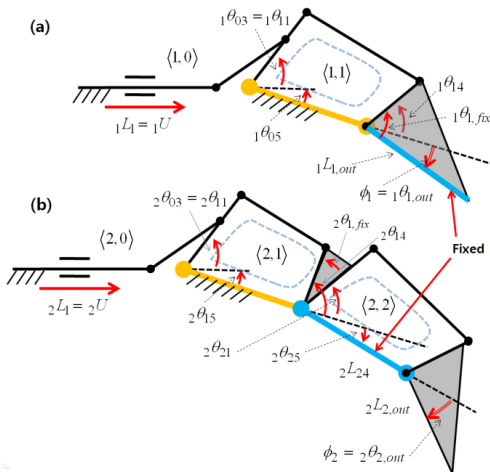


Fig. 7. 2 DOF manipulator

First, in order to make 2 DOF robotic manipulator, two mechanism planes in Fig. 7 should be stacked and tied together at

the links ${}_1L_{1,out}$ and ${}_2L_{24}$. Also, if the base link ${}_1L_{14}$ of 4-BAR of first mechanism plane is earthed to the ground, then we can obtain the following relation from the first mechanism plane like Eq. (14):

$$\dot{\phi}_1 = \begin{bmatrix} {}_1\dot{\theta}_{14} \end{bmatrix} = \begin{bmatrix} {}_1\mathbf{Q}_{1(3,1)} \end{bmatrix} \begin{bmatrix} {}_1\dot{\theta}_{11} \end{bmatrix} \quad (18)$$

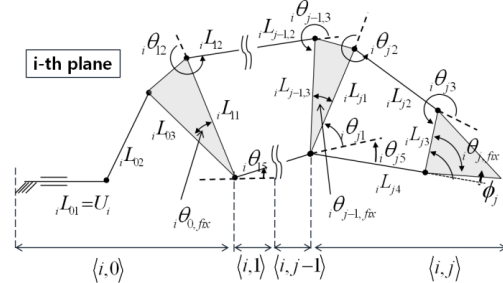


Fig. 8. i -th mechanism plane

Fig. 7(b) illustrates the second mechanism plane to be stacked to first mechanism plane. Also, since the 4-BAR $\langle 2,2 \rangle$ is not earthed to the ground, the output is obtained as follow:

$$\begin{bmatrix} \dot{\phi}_2 \end{bmatrix} = \begin{bmatrix} {}_2\dot{\theta}_{24} \end{bmatrix} = \begin{bmatrix} {}_2\mathbf{Q}_{2(3,1)} & {}_2\mathbf{Q}_{2(3,2)} \end{bmatrix} \begin{bmatrix} {}_2\dot{\theta}_{21} \\ {}_2\dot{\theta}_{25} \end{bmatrix}, \quad (19)$$

where ${}_2\dot{\theta}_{25}$ is the virtual active joint. On the other hand, ${}_2L_{14}$ is earthed to the ground as show in Fig. 7(b), we have the following relation:

$$\begin{bmatrix} {}_2\dot{\theta}_{14} \end{bmatrix} = \begin{bmatrix} {}_2\mathbf{Q}_{1(3,1)} \end{bmatrix} \begin{bmatrix} {}_2\dot{\theta}_{11} \end{bmatrix} \quad (20)$$

In addition, we can get the following two relations from the Fig. 7(b):

$${}_2\theta_{21} = {}_2\theta_{14} - {}_2\theta_{1,fix}, \quad (21)$$

and

$${}_2\dot{\theta}_{21} = {}_2\dot{\theta}_{14}. \quad (22)$$

By applying Eq. (20) and (22) to (19), we can obtain the following equation:

$$\begin{bmatrix} \dot{\phi}_2 \end{bmatrix} = \begin{bmatrix} {}_2\mathbf{Q}_{2(3,2)} & {}_2\mathbf{Q}_{2(3,1)} \end{bmatrix} \begin{bmatrix} 1 & 0 \\ 0 & {}_2\mathbf{Q}_{1(3,1)} \end{bmatrix} \begin{bmatrix} {}_2\dot{\theta}_{25} \\ {}_2\dot{\theta}_{11} \end{bmatrix}. \quad (23)$$

From above Eq. (23), we can know that the second mechanism plane shown in Fig. 7(b) seems to have two input variables and one output variable. However, ${}_2\theta_{25}$ is the virtual input variable which can be replaced with the function of ${}_1\theta_{11}$ of first mechanism plane, because two mechanism planes are stacked and tied together at the links ${}_1L_{1,out}$ and ${}_2L_{24}$. In other words, the virtual input is determined by the output of the first plane. As a result, we can get the following relation:

$$\begin{bmatrix} \dot{\phi}_1 \\ \dot{\phi}_2 \end{bmatrix} = \begin{bmatrix} 1 & 0 \\ {}_2\mathbf{Q}_{2(3,2)} & {}_2\mathbf{Q}_{2(3,1)} \end{bmatrix} \begin{bmatrix} {}_1\mathbf{Q}_{1(3,1)} & 0 \\ 0 & {}_2\mathbf{Q}_{1(3,1)} \end{bmatrix} \begin{bmatrix} {}_1\dot{\theta}_{11} \\ {}_2\dot{\theta}_{11} \end{bmatrix}. \quad (24)$$

Also, above Eq. (24) can be rewritten as following compact form:

$$\begin{bmatrix} \dot{\phi}_1 \\ \dot{\phi}_2 \end{bmatrix} = [G_2] \begin{bmatrix} \dot{\theta}_{11} \\ \dot{\theta}_{21} \end{bmatrix}, \quad (25)$$

where $[G_2]$ is the rate kinematic relation of the 2-DOF stackable mechanisms without the input mechanisms as shown in Fig 7. As we can see in Eq. (25), two output variables are related with two input variables. That is, if the first mechanism plane with one 4-BAR is stacked with the second mechanism plane composed of two 4-BARs, then the stacked mechanisms can be a complete 2-DOF robotic manipulator system. Moreover, if the input mechanism of each plane is applied to Eq. (25), then we can get the resultant equation as following form:

$$\begin{bmatrix} \dot{\phi}_1 \\ \dot{\phi}_2 \end{bmatrix} = [G_2] \begin{bmatrix} {}_1G_0 & 0 \\ 0 & {}_2G_0 \end{bmatrix} \begin{bmatrix} {}_1\dot{U} \\ {}_2\dot{U} \end{bmatrix}. \quad (26)$$

Also, without loss of generality, the rate kinematics can be extended to the N-DOF manipulator as follow:

$$\begin{bmatrix} \dot{\phi}_1 \\ \dot{\phi}_2 \\ \vdots \\ \dot{\phi}_n \end{bmatrix} = [G_n] \begin{bmatrix} {}_1G_0 & & & \\ & {}_2G_0 & & \\ & & \ddots & \\ & & & {}_nG_0 \end{bmatrix} \begin{bmatrix} {}_1\dot{U} \\ {}_2\dot{U} \\ \vdots \\ {}_n\dot{U} \end{bmatrix} \quad (27)$$

Till now, we have suggested the rate kinematics of the proposed robotic manipulator by using new stackable 4-BAR mechanisms. The simulation results will be discussed in the following section.

IV. SIMULATION AND PROTOTYPE

To verify the applicability of suggested manipulator, we are to show both simulation results and prototype. The simulation is performed by using commercial dynamic simulation SW DAFUL (by VirtualMotion Co.) and MatLab (by MathWork Co.). Also, a prototype manufacturing will show the concept of the suggested manipulator using the stackable mechanisms.

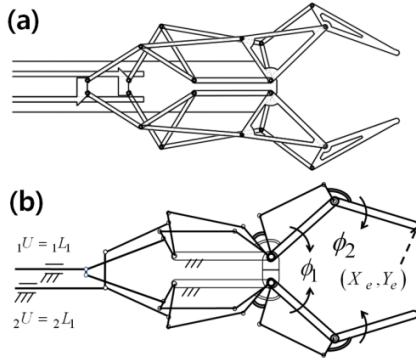


Fig. 9. Simulation model

A. Simulation

Fig. 9(a) illustrates the simulation model of 2-DOF gripper using the stackable mechanisms. More detail, the simulation model is composed of the four working joints and two actuators but each finger is operated symmetrically as shown in Fig. 9(b). The Fig. 10 shows that the gripper can generate a variety of motions. As we can see in this simulation, the proposed 2-DOF gripper does not require the actuators to attach directly to driving joints and it

can be independently controlled.

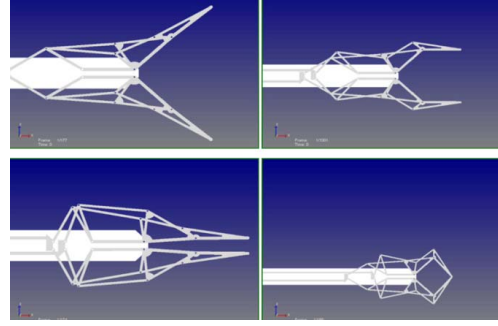


Fig. 10. Simulation result using DAFUL SW

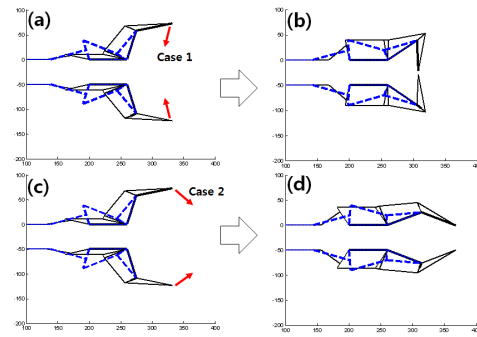
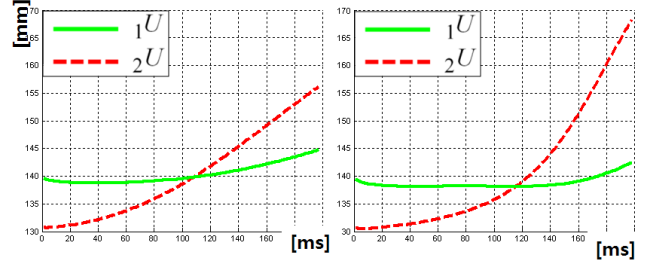


Fig 11. Simulation procedures



(a)Case 1 (b) Case 2
Fig 12. Simulation result by MatLab SW

In Eq. (26), we have suggested the velocity relation between the inputs of actuators and the outputs of working joints. Here, the end-effector of 2-DOF gripper can be controlled in the Cartesian space by using a conventional Jacobian matrix of serial 2-DOF manipulator like this:

$$\begin{bmatrix} \dot{X}_e \\ \dot{Y}_e \end{bmatrix} = [J]^{-1} [G_2] \begin{bmatrix} {}_1G_0 & 0 \\ 0 & {}_2G_0 \end{bmatrix} \begin{bmatrix} {}_1\dot{U} \\ {}_2\dot{U} \end{bmatrix}, \quad (28)$$

where $[J]$ is the Jacobian matrix of a 2-DOF planner serial manipulator, $[G_2]$ is the velocity relation of 2-DOF stackable mechanisms, and ${}_1G_0$ and ${}_2G_0$ are the velocity relation of the input mechanisms, respectively. Fig. 11 illustrates the simulation procedures using MatLab; the Fig. 11(a) and (c) are the initial configurations. According to target motions (case 1 and 2 in Fig. 11), the 2-DOF gripper could be manipulated as shown in Fig. 11(b) and (d), respectively. Also, the actuator inputs of case 1 and 2 were generated as

shown in Fig. 12 (a) and (b).

B. Prototype

A prototype of 3-DOF manipulator has been suggested to show the applicability of the proposed stackable mechanisms. The actuators could be separated from the suggested manipulator as shown in Fig. 13. Thus the small-size and light-weight 3-DOF manipulator is successfully made without any electrical components such as wiring or motors. In this 3-DOF manipulator shown in Fig. 13, 2-DOF manipulator makes use of the suggested stackable mechanisms and 1-DOF gripper utilizes the conventional wire-driven mechanism. Also, the passageway of wire for gripper was suggested in Fig. 13(b) and (c). The prototype is manufactured to be manually operated without actuators. Also, this prototype shows that the suggested stackable mechanism can be made as small-size, moreover it is able to offer passageway for the wire driven within stackable mechanism. Finally, Fig. 14 shows a few motion snapshots of the suggested prototype. The suggested prototype was manufactured to show the possibility as a new manipulator for surgical robot. The conventional manipulator of surgical robot such as DaVinci makes use of wire-driven mechanism for motion generations, but the wire-driven method cannot support a large force for the surgery. However, since the 4-BAR mechanism is based on the parallel mechanism, the suggested manipulator using stackable 4-BAR mechanisms can support a large force comparing to the wire-driven method. Also, since the suggested method can separate the electrical system from the manipulator, it can be used in the Magnetic Resonance Imaging (MRI) environment without electrical damages. In other words, the suggested manipulator using stackable mechanisms can be used in a special environment including various field robots.

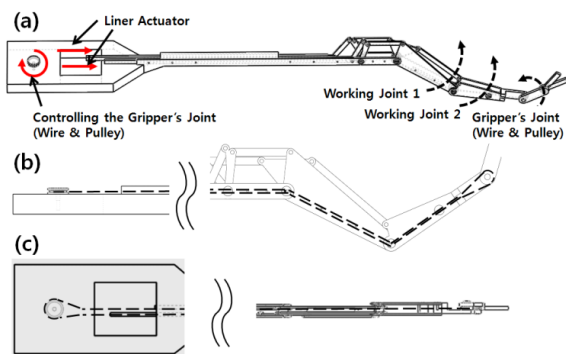


Fig. 13. Prototype of the suggested 3-DOF manipulator (2-DOF stackable, 1-DOF Wire-Driven)

V. CONCLUSION

The new planar robotic manipulator using stackable 4-BAR mechanisms has been proposed and analyzed in this paper. The suggested mechanism was able to separate the electrical component from the mechanical linkage/joint components in the robotic manipulator. Thus the robotic manipulator

including working joints and linkages could be manufactured using one material with light-weight and slim-size. Through simulation and the prototype of manipulator, we have shown its applicability to robotic manipulator with special purpose, such as the manipulator of surgical robot or manipulator of field robot which is required actuators to be separated from the manipulator.

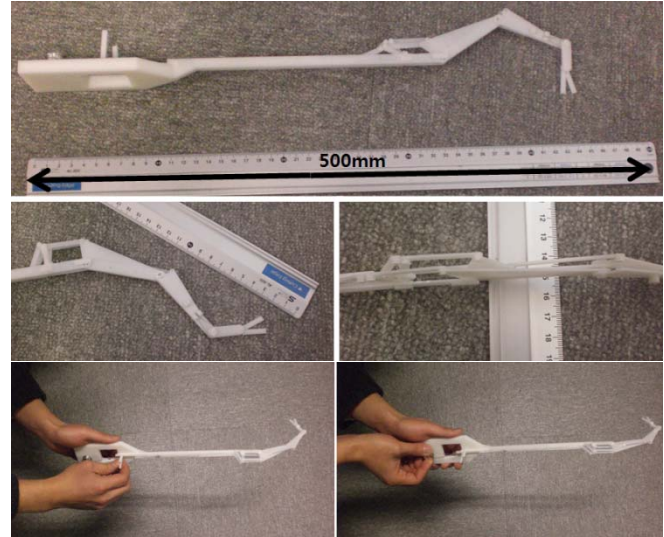


Fig. 14. Snapshots of 3-DOF manipulator

REFERENCES

- [1] H.-S. Yoon and B.-J. Yi, "A 4-DOF Flexible Continuum Robot Using a Spring Backbone," IEEE Int. Conf. on Mechatronics and Automation, pp. 1249-1254, Aug., 2009.
- [2] K. Xu, R. E. Goldman, J. Ding, P. K. Allen, D. L. Fowler and N. Simaan, "System Design of an Insertable Robotic Effector Platform for Single Port Access (SPA) Surgery," International Conference on Intelligent Robots and Systems, pp.5546-5552, Oct., 2009.
- [3] K. Tadano¹, W. Suminol, K. Kawashima¹, and T. Kagawa¹, "Pneumatically Driven Forceps Manipulator for Laparoscopic Surgery," SICE Annual Conference, pp.2993-2996, Aug., 2008.
- [4] <http://www.bostondynamics.com>
- [5] L. Birglen and C. M. Gosselin, "Force Analysis of Connected Differential Mechanisms: Application to Grasping," International Journal of Robotics Research, vol.25, No.10, pp.1033-1046, 2006.
- [6] K. Chinzei, and K. Miller, "MRI Guided Surgical Robot," Australian Conference on Robotics and Automation, Sydney, pp.50-55, Nov., 2001.
- [7] B.-J. Yi and R. A. Freeman, "Geometric Analysis of Antagonistic Stiffness in Redundantly Actuated Parallel Mechanisms," Journal of Robotic Systems, vol. 117, pp. 10-16, Sep., 1993
- [8] J.-P. Merlet, Parallel robots, Springer, 2006.
- [9] J. Angeles, and M. Callejas, "An Algebraic Formulation of Grashof's Mobility Criteria with Application to Linkage Optimization Using Gradient- Dependent Methods," ASME J. Mech., Transmission, and Automation in Design, vol. 106, No. 3, pp.327-332, Dec. 1984.
- [10] B.-J. Yi, S.-R. Oh, and I.-H. Suh, "A Five-Bar Finger Mechanism Involving Redundant Actuators: Analysis and Its Applications", IEEE Trans. Robotics and Automation, vol. 15, No. 6, pp.1001-1010, Dec. 1999.
- [11] J.-H. Lee, B.-J. Yi, S.-R. Oh, and I.-H. Suh, "Optimal design and development of a five-bar finger with redundant actuation", Mechatronics, vol. 11, No. 1, pp. 27-42, 2001.
- [12] J. Chung, B.-J. Yi, and S. Oh, "Design of a New Spatial 3-DOF Parallel Mechanism with Application to a Flat Panel TV Mounting Device," IEEE Trans. Robotics, Vol. 25, No. 5, pp.1214-1221, Oct. 2009.